

# VSA-II: a Novel Prototype of Variable Stiffness Actuator for Safe and Performing Robots Interacting with Humans

R. Schiavi, G. Grioli, S. Sen, A. Bicchi

Interdepartmental Research Center “E. Piaggio”

Faculty of Engineering, University of Pisa via Diotisalvi,2 56100, Pisa (Italy)

{riccardo.schiavi,giorgio.grioli,soumen.sen,bicchi}@ing.unipi.it

**Abstract**—This paper presents design and performance of a novel joint based actuator for a robot run by Variable Stiffness Actuation, meant for systems physically interacting with humans. This new actuator prototype (VSA-II) is developed as an improvement over our previously developed one reported in [9], where an optimal mechanical-control co-design principle established in [7] is followed as well. While the first version was built in a way to demonstrate effectiveness of Variable Impedance Actuation (VIA), it had limitations in torque capacities, life cycle and implementability in a real robot. VSA-II overcomes the problem of implementability with higher capacities and robustness in design for longer life. The paper discusses design and stiffness behaviour of VSA-II in theory and experiments. A comparison of stiffness characteristics between the two actuator is discussed, highlighting the advantages of the new design. A simple, but effective PD scheme is employed to independently control joint-stiffness and joint-position of a 1-link arm. Finally, results from performed impact tests of 1-link arm are reported, showing the effectiveness of stiffness variation in controlling value of a safety metric.

**Index Terms**—Physical Human-Robot Interaction, Safety, Performance, Variable Stiffness Mechanisms, Actuators

## I. INTRODUCTION

Robots meant for physical Human-Robot Interaction (pHRI) must remain safe against all possible circumstances, including unexpected impacts. Automotive industry considers impact on human head as the most susceptible to serious injury and literature presents a well developed metric on this class of injury. Recently Haddadin et al. in [16] has carried out, for the first time in robotics, extensive impact tests by a robot on standard dummies, in a way to find an effective safety measure relevant to physical human robot interaction. Though the study by Haddadin et al. indicates ineffectiveness of injury criteria developed for automobiles, however, in order to have reasonableness, in this discussion, an acceleration based injury metric, as developed in [4] is considered. The level of acceleration of the impacted body is highly influenced by the inertia of impacting body (robot). The above said safety criterion, namely, Head Injury Coefficient (*HIC*) very well captures this inertia effect.

Ensured safety taken granted, the second most important attribute of a robot is its performance. While performance is a complex set of attributes such as software dependability, hardware reliability, etc. ([1], [3]), we will only consider a basic aspect of performance, namely velocity of motion.

Traditional design have attempted to see safety and performance as two distinct aspects. There are many instances where constant compliance in transmissions between actuator and robot link is introduced to attenuate the reflected inertia of the motor such as in [15] in order to reduce the effect of impact. Introduction of constant compliance has the inevitable effect of reduction in performance bandwidth. In recent past, works of Bicchi et al. ([5], [6], [7]) and Zinn et al. ([8]) have opened up new directions, where a robotic manipulator is designed and/or optimally controlled to recover the lost performance in presence of compliance for intrinsic safety. A paradigm shift thus gets established “design for safety and control for performance”.

In this new direction [7] presents a time optimal control problem for performance, ensuring safety in terms of unexpected impact. This leads to an actuation method, called *Variable Stiffness Approach* and its generalized form as *Variable Impedance Approach*, where the stiffness/impedance of the transmission between prime mover and actuated link gets varied. The outcome is a new paradigm of robot action, *Stiff-&-Slow* and *Soft-&-Fast* operation.

The necessary simultaneous control of motion and stiffness can be achieved by explicit stiffness control. An alternative to this, encouraged by biological designs, is using two motors antagonistically, via use of so called *non-linear spring* as an elastic transmission between each of the motors and the actuated link. In [9], [10], [11] the concept of antagonistic actuation has been analysed in theory and implemented in its first prototype, namely Variable Stiffness Actuator-1 (VSA-I). VSA-I as a demonstrator for variable stiffness actuation has established the principle and purpose. However, It finds limitation in torque capacity and in practical implementation in a robotic arm. This paper presents an improved design and development of VSA-II on simpler antagonistic concept for a direct robotic joint actuation. It discusses, in detail the VSA-II mechanism, the stiffness characteristics and comparative performances between VSA-I and VSA-II.

The article is structured as follows: section II describes design of VSA and its stiffness characteristics, section III says about the dynamics and control of VSA, while section IV illustrates few aspects of VSA-II as compared to VSA-I. Section V describes the experimental set up and the results obtained there on. Finally conclusions are drawn in section VI.

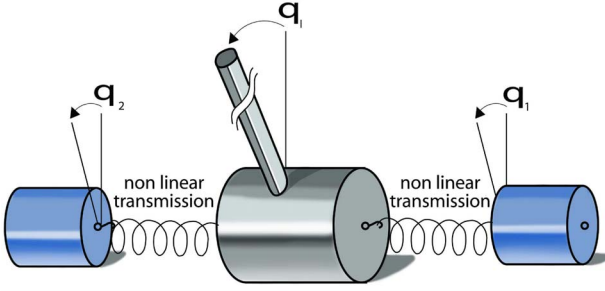


Fig. 1. VSA-II schematic.  $q_1$  and  $q_2$  are angle of the motors,  $q_1$  id the joint shaft displacement.

## II. DESIGN OF VSA-II

The new prototype of Variable Stiffness Actuator, VSA-II, is conceived to improve over the previous prototype to have an increased torque capacity in a more compact assembly, in order to use it as a joint actuator for a robotic arm.

In VSA-I (see [9]) a timing belt was used which had a limited load capacity, and a short life cycle. The VSA-II transmission system is based on 4-bar mechanisms which show more robustness and larger load bearing capacity.

The aim of the transmission system is to get a non linear torque-displacement characteristic between the input torque applied by the motors and the angular deflection of the joint shaft. The well known 4-bar mechanism can be suitably designed to have desired transmission ratio between input and output. Employing a simple linear spring on the input, the relationship between deflection and torque on the output shaft can be made non-linear.

### A. 4-bar spring mechanism

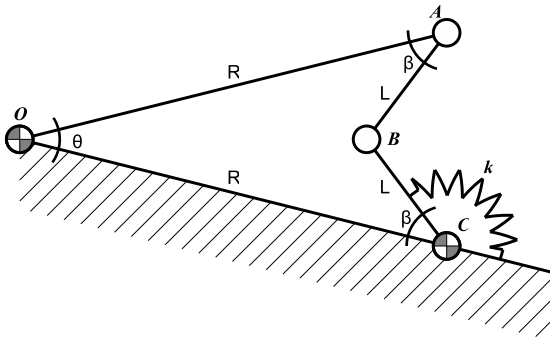


Fig. 2. Line diagram of 4-bar transmission mechanism of VSA II. Link  $\overline{OA}$  of length  $R$  is driven by a motor at  $O$ . The torque spring  $k$  has a linear behaviour. Stiffness seen at  $O$  attains non-linearity through the geometry, where angle  $\theta$  at  $O$  and transmission angle  $\beta$  are related non-linearly.

The designed 4-bar mechanism (see Fig.2) is a special case of Grashof 4-bar linkage, or, so called *Grashof neutral linkage*, having two equal shortest links ( $\overline{AB}$  and  $\overline{BC}$ ) and two equal longest links ( $\overline{OA}$  and  $\overline{OC}$ ). Basically, it is a crank-rocker mechanism with  $\overline{BC}$  as input link and  $\overline{OC}$  as ground, or, a double-rocker mechanism, seen from link  $\overline{OA}$  (the coupler  $\overline{AB}$  can have full rotation, see [12], [13] ).

Link  $\overline{OA}$  is connected to a motor at  $O$  and has angular movement  $\theta$  with respect to ground link  $\overline{OC}$ . Link  $\overline{BC}$  is loaded by a *linear torque spring* at  $C$ , where  $\beta$  is the transmission angle at  $A$ . By designing the link lengths suitably, it is possible to have desired non-linear relationship between input and output link angles. It is to be noted that the non-linearity lies only in the geometry and the mechanism behaves as a non-linear elastic transmission element to the purpose of our application. The torsional spring  $k$  is set to be at zero equilibrium with  $\theta = \beta = 0$ . The output angle range is  $\theta \in [-\theta_{MAX}; \theta_{MAX}]$ . To ensure not to cross the singularity configuration at  $\theta = 0$ , a mechanical stop is employed, reducing the range to  $\theta \in (0; \theta_{MAX}]$ . From geometry,  $\theta_{MAX} = 2 \arcsin(L/R)$ .

As shown in the Fig.2 and using properties of triangle we can write

$$\beta = \arcsin\left(\frac{R}{L} \sin\left(\frac{\theta}{2}\right)\right) - \frac{\theta}{2}. \quad (1)$$

The potential energy stored in the spring is  $P = 1/2k\beta^2$ , and the torque at the motor end  $O$  due to deflection  $\beta$  on torque spring is only a function of geometry and is expressed as

$$M(\theta) = \frac{\partial P}{\partial \theta} = \frac{1}{2}k\beta \left( \frac{\frac{R}{L} \cos \frac{\theta}{2}}{\sqrt{1 - \left(\frac{R}{L} \sin \frac{\theta}{2}\right)^2}} - 1 \right). \quad (2)$$

Similarly, the stiffness seen at  $O$  on link  $\overline{OA}$  can be derived to be

$$\sigma(\theta) = \frac{\partial^2 P}{\partial \theta^2} = \frac{1}{4}k \left[ \left( \frac{\frac{R}{L} \cos \frac{\theta}{2}}{\sqrt{1 - \left(\frac{R}{L} \sin \frac{\theta}{2}\right)^2}} - 1 \right)^2 + \frac{\frac{R}{L} \left(\frac{R}{L}^2 - 1\right) \beta \sin \frac{\theta}{2}}{\left[1 - \left(\frac{R}{L} \sin \frac{\theta}{2}\right)^2\right]^{\frac{3}{2}}} \right]. \quad (3)$$

The ratio  $\frac{R}{L}$  and the spring constant  $k$  are the two design parameters. These parameters are to be judiciously decided depending on desired torque capacity and deflection range. As shown in Fig.3 the deflection range increases with smaller  $\frac{R}{L}$  ratio.

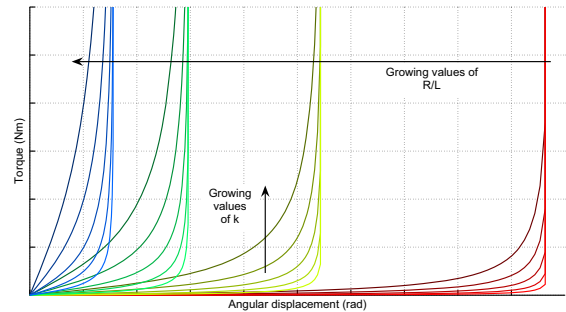


Fig. 3. Theoretical torque deflection characteristics can be obtained with various values of  $R/L$  and  $k$  for  $\theta \geq 0$  (curves are symmetric with respect to the origin). The effect of  $k$  is to scale the overall function. Graphs are plotted for  $k = 20, 40, 80, 160, 320$  Nm/rad.

### B. Stiffness characteristic

VSA-II is essentially an antagonistic actuator having two motors in opposition (Fig.1). Core of VSA-II assembly consists of two pairs of 4-bar mechanisms where each pair on either side is associated with a motor. Referring to Fig.1  $q_1$  and  $q_2$  are the angles of the motors, and  $q_l$  is the link position. Defining  $\theta_{i,j} = q_i - q_j$  the load torque expression is

$$\tau_l = 2M(\theta_{1,l}) + 2M(\theta_{2,l}) = 2M_{1,l} + 2M_{2,l},$$

and the stiffness expression  $\sigma$  is

$$\sigma = \frac{\partial \tau_l}{\partial q_l} = 2\sigma_{1,l} + 2\sigma_{2,l}. \quad (4)$$

Fig.4 shows the stiffness function of VSA-II with varying

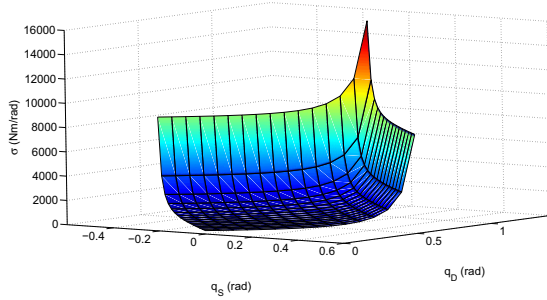


Fig. 4. VSA-II stiffness for joint shaft position  $q_l = 0$  varying  $q_S$  and  $q_D$  in the admissible range.

$q_S = (q_1 + q_2)/2$  and  $q_D = (q_1 - q_2)/2$  maintaining  $q_l = 0$ , where  $q_S$  corresponds to the motor mean position and  $q_D$  relates to stiffness. It can be noticed that the stiffness grows to infinity with  $q_D$  (fig 4).

### III. DYNAMICS AND CONTROL OF VSA-II SYSTEM

In this section we discuss the dynamics and control of a 1-DOF experimental set-up constituted of a VSA-II actuated link. We propose an easy but effective control scheme, to be able to independently vary stiffness and position of the joint shaft as followed in [9].

The dynamics of the system can be expressed as

$$\begin{cases} I_r \ddot{q}_1 + B \dot{q}_1 = 2M_{1,l} + \tau_1 \\ I_r \ddot{q}_2 + B \dot{q}_2 = 2M_{2,l} + \tau_2 \\ J \ddot{q}_l + B \dot{q}_l + mgD \sin q_l = -2(M_{1,l} + 2M_{2,l}) - \tau_{load} \end{cases} \quad (5)$$

where  $m$  and  $D$  are the mass and length of the link,  $I_r$  and  $J$  are the DC motors and link rotary inertia, respectively,  $B$  is the (small) axial damping coefficient, and  $M_{a,b}$  are the torques generated on the pulleys by the 4-bar mechanisms (see section II). The term  $\tau_{load}$  collects external disturbances acting on the link, while  $\tau_1, \tau_2$  are the control torques acting on the two electric motors.

In steady state equilibrium, under negligible gravity and disturbance torque, link position becomes  $q_l = (q_1 + q_2)/2 = q_S$  and the joint stiffness holds as a function of differential position of the motors,  $q_D$ . This suggests the control task

to independently control the joint shaft position  $q_l$  and the transmission stiffness  $\sigma$  by controlling the angles  $q_S$  and  $q_D$ .

Introducing the state variables  $(q_S, q_D, \dot{q}_S, \dot{q}_D)$ , the system dynamics in 5 can be rearranged by simply adding and subtracting the first and second, to read

$$\begin{cases} I_r \ddot{q}_S + B \dot{q}_S = 2M_S + \tau_S \\ I_r \ddot{q}_D + B \dot{q}_D = 2M_D + \tau_D \\ J \ddot{q}_l + B \dot{q}_l + mgL \sin(q_l) = -4M_S - \tau_{load} \end{cases} \quad (6)$$

where, in particular,  $M_S = (M_{1,L} + M_{2,L})/2$ ,  $M_D = (M_{1,L} - M_{2,L})/2$ , and  $\tau_s = (\tau_1 + \tau_2)/2$ ,  $\tau_d = (\tau_1 - \tau_2)/2$  are the respective control torques.

The control implemented is basically a PD scheme in anticipation that the use of a PID in the control could neutralize the benefits of the variable stiffness in case of accidental impact. Gravity compensation should be added when operation in a non horizontal plane is considered. The control scheme is the one in Fig.5, showing the de-coupling between the link and the stiffness dynamics. There are two separate control loops, one of which operates on  $\tau_S$  feeding back the error on  $q_l$ , while the other one operates on the  $\tau_D$  feeding back the error on  $q_D$ .

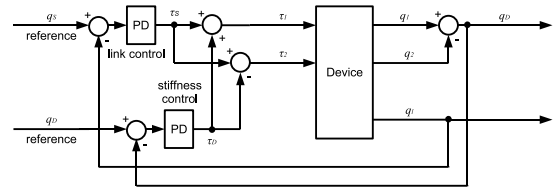


Fig. 5. Control scheme used.

### IV. DESIGN COMPARISON

In this section we compare VSA-I and VSA-II designs from a theoretical perspective. First difference lies in the design; the VSA-I has cross-coupling between the motors, whereas VSA-II implements a simple antagonistic arrangement, being less complex in parameters optimization. It is clear that the motor torques gets distributed in stiffness generation and resultant joint torque and this distribution is different for the two prototypes. VSA-I needs differential angle between the two actuators to obtain minimum stiffness. A differential torque  $\tau_D$  is needed to generate that angle reducing the available torque for motion. For the VSA-II the minimum stiffness is obtained for  $q_D = 0$  ( $\tau_D = 0$ ), as shown in Fig.6,

VSA-I and II have different stiffness ranges. If the devices are actuated by motors with limited torques, the feasible stiffness range gets limited because infinite stiffness condition would also require infinite torque. The motors also have to balance the external disturbance torque on the link  $\tau_{load}$ , reducing the torque available for stiffness control.

Fig. 7 shows how the different designs of VSA-I and II affects the stiffness range. In both devices the effect of increasing external load is to decrease the stiffness range. The major difference between the two behaviours is that

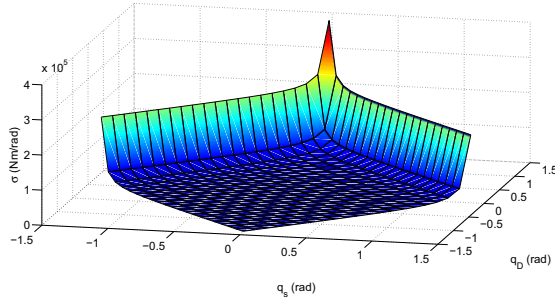


Fig. 6. VSA-I stiffness for joint shaft position  $q_l = 0$  varying  $q_S$  and  $q_D$  in the admissible range.  $q_S$  and  $q_D$  have similar definitions.

while in VSA-I, increasing external torque will induce higher maximum stiffness, in VSA-II any increment in  $\tau_{load}$  makes the maximum stiffness decrease. In case of impact, the transmission is desired to be as compliant as possible to be safe. While the reaction torque on the link can increase the maximum stiffness of VSA-I, in contrary it always decreases the maximum stiffness of VSA-II. In VSA-II the maximum stiffness is limited by motor's stall torque while in VSA-I it depends also on the applied load.

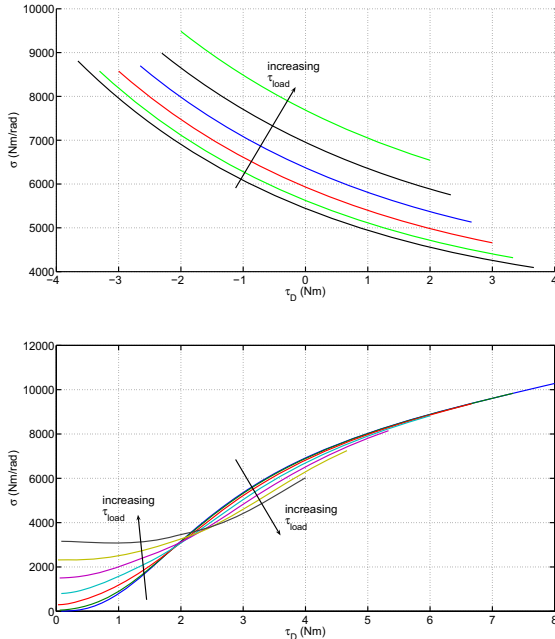


Fig. 7. Stiffness - torque relationship for VSA-I (top) and VSA-II (bottom). The plots show the stiffness seen from the link as a function of the differential torque  $\tau_D$ , for increasing values of external disturbance torque on the link  $\tau_{load}$ . Curves are obtained with limited torque  $\tau_{MAX} = 4.356$  for the motors, and external load torque  $\tau_D = \{0, 0.66, 1.33, 2, 2.66, 3.33, 4\}$ .

Important parameters to appraise performances of VSA actuators are the midpoint of the stiffness range  $\sigma_m$  and the relative amplitude  $\Delta_\sigma = (\sigma_{MAX} - \sigma_{MIN})/2\sigma_m$ . Fig. 8 shows that  $\Delta_\sigma$  has larger values on the VSA-II giving rise to better performance as explained in [7].

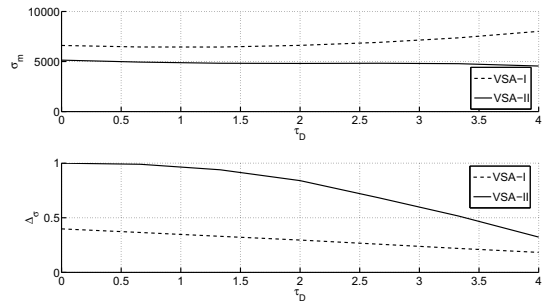


Fig. 8. Trends of  $\sigma_m$  and  $\Delta_\sigma$ , for VSA-I and II obtained from data in Fig.7.

## V. EXPERIMENTS

### A. Setup

Experimental results on VSA-II prototype are reported here. The prototype is designed and developed based on the principles delineated in the previous sections. The prototype has two elastic elements for each side consisting of four 4-bar mechanisms. This leads to symmetric loading on bearings, structure and springs. The two sides of the device are rotated of 90 deg to achieve a more compact design.

The overall length and radius of the prototype are 85mm and 60mm respectively. It is fabricated using aluminium for the main structure, steel and bronze for the spindles and bushes, and spring steel for the springs. The total weight of the prototype is 0.345Kg. Each spring has a nominal torsional stiffness of  $k = 0.5$  Nm/rad, and the ratio  $R/L$  is 14/8. The prototype is shown in Fig. 9. Te device is actuated



Fig. 9. VSA-II prototype, open up. The prototype integrates the non-linear elements needed to obtain the variable stiffness. It is composed of two equal halves, each half contains two 4-bar mechanism to allow internal stress to be distributed more evenly along the structure.

by two motors (Faulhaber 3257G024CR-32/3), with stall torque 14.7Nm, maximum speed of 44rpm at the gearhead output, where the ratio is 134 : 1. The link is an aluminium bar of length 170mm and mass 0.135Kg.

The sensors used are three optical incremental encoders (HP HEDS-5500) with resolution 500cpr, two of them are

fixed to the motor axes, while the third one is connected to the link.

### B. Experiments

Here we report results of experiments conducted with VSA-II, in actuating a simple 1-DOF planar link (Fig.10). The implemented control shows trajectory tracking at speed

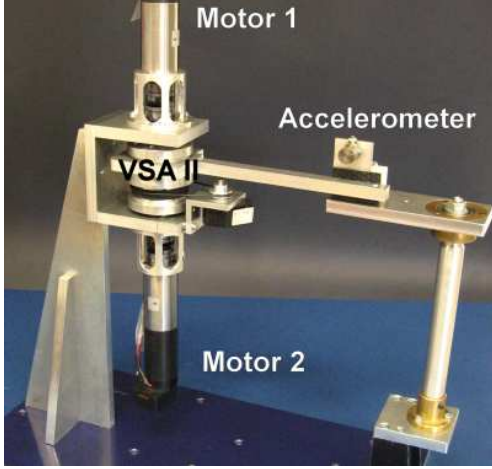


Fig. 10. Experimental set-up for calibration and impact tests.

up to 2.5rad/s; an example trajectory following is shown in Fig.11. To demonstrate the effectiveness of the new prototype

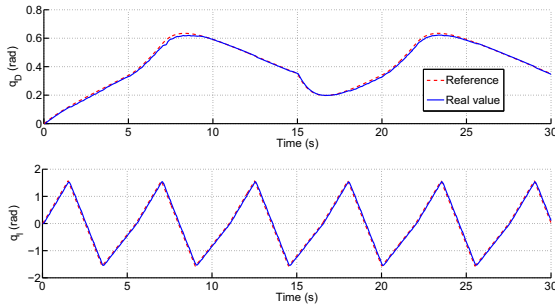


Fig. 11. Trajectory following with the implemented PD control system (reference dashed, trajectory solid).

we performed several experiments. Stiffness calibration and impact tests are reported.

1) *Stiffness measurement:* To determine the torque-deflection characteristics (Fig.12) on variations of the differential position of the two motors  $q_D$ , known external loads have been applied and encoder readings were recorded, the slightly asymmetric behaviour is due to small differences between the elastic elements. Fig.12 shows the average torques against link positions with various  $q_D$ , obtained performing various calibration cycles. Fig. 13 illustrates the derived stiffness characteristic. As expected the stiffness values increase for growing values of  $q_D$ .

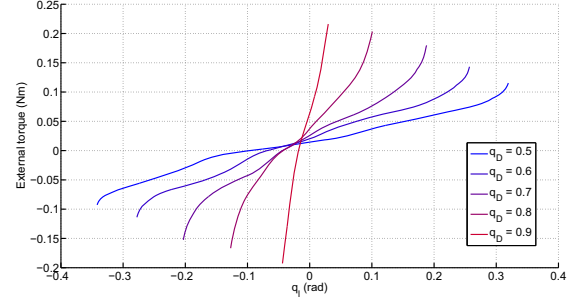


Fig. 12. Average torque vs displacement plot, for VSA II. The relationship between the link displacement and the reaction-force is evident in the figure. The asymmetrical behaviour is due to imperfect matching between the springs in the prototype.

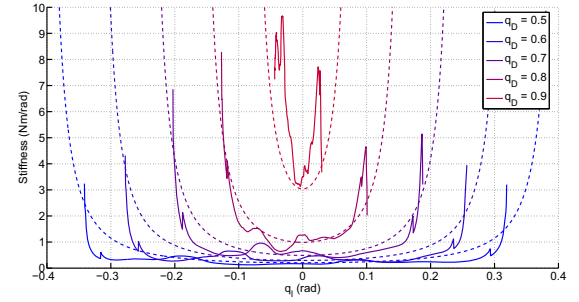


Fig. 13. Stiffness vs displacement plot, theoretical (dashed) and experimental (solid). Larger differential angles make the mechanism stiffer.

2) *Impact tests:* The effectiveness of the device was tested under impacts against a body of known mass. A piezo-accelerometer (model 4371 Brüel and Kjær) was mounted on the probe mass, that was free to move in a horizontal plain about an axis. The end point of the link on VSA II was actuated to impact against the mass. Different values of joint shaft stiffness were set and the impact tests were carried out at constant velocity, recording the resulting acceleration of the mass.

To correlate the safety level with impact the standard injury criterion, Head Injury Coefficient (HIC) is adopted in this study, following the derivations in [4]. The HIC is defined as

$$HIC = \max_{T_{MAX}} \left\{ (t_2 - t_1) \left[ \frac{1}{t_2 - t_1} \int_{t_1}^{t_2} |a(t)| dt \right]^{2.5} \right\},$$

$$0 \leq t_1 \leq t_2 \leq T_{max},$$

where  $T_{MAX}$  is the time duration of the impact,  $a(t)$  is the acceleration of the impacted mass, measured in  $g$  (acceleration due to gravity). HIC values obtained in the tests do not correspond to any severity level in standard scales, because the probe mass used was not standardized with respect to a human head, but just a scaled down version. The experiment showed particularly low values of HIC also because of low motor and link inertias. Anyhow the collected data can be accepted as a relative metric to compare crashes happening at different conditions. For each set stiffness several tests were performed and average values are considered. Fig.14 shows

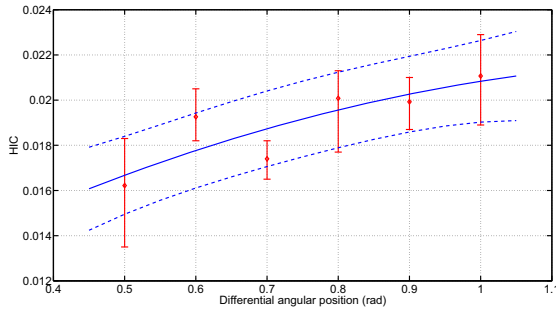


Fig. 14. Experimental values HIC vs differential angular position, with fitting polynomial. Lower values of stiffness, tend to get lower values of HIC and so are safer.

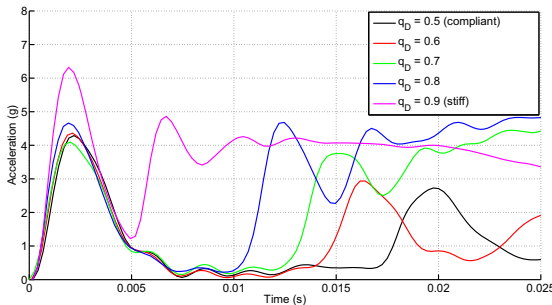


Fig. 15. Acceleration of the impacted body during different impact test with different stiffness levels, it can be noticed the separation between the contribution to the impact due to the link mass (the first peak of the profiles) and the contribution due to the motor and gears inertia (the second peak, which happens later in time for compliant configurations and sooner for stiff configurations).

the scatter plot of average and minimum-maximum values. Data were interpolated using a second order polynomial, to show the main trend. We can notice that lower values of stiffness grant lower HIC values and thus better safety. This happens because lower stiffness decouples more effectively the rotor from the link inertia. The acceleration profiles after impact are showed in Fig.15, where the distinct contributions of rotor inertia and link inertia with time can be noticed.

## VI. CONCLUSIONS AND FUTURE WORK

In this paper we discussed the design and control of an actuator to be used in machines and robots physically interacting with humans, implementing criteria established in [7] for an optimal, intrinsically safe, yet performing machine. An implementation of such concepts, consisting of a novel Variable Stiffness Actuation (VSA) joint, that improves a previous implementation was described. The design and the working principle of the VSA-II were reported. A short comparison between the theoretical performances of VSA-I and II was discussed. The analysis of the VSA-II dynamic behaviour was presented, along with a simple but effective control scheme. It is concluded that VSA-II shows higher torque capacity and behaves in a better way with respect to stiffness behaviour when undergoes impact. Finally, experimental results showing performance and safety of a one-link arm actuated by the VSA motor were reported.

Future work will address further improvement of the VSA-class of actuators, for what concerns stiffness range, encumbrance and weight reduction, etc. Moreover an integrated design of a 3-DOF variable stiffness arm is undergoing.

## VII. ACKNOWLEDGMENTS

The Variable Stiffness Actuation approach is patented. Authors would like to acknowledge the work done by Gianluca Boccadamo, Davide Decarli, and Dr. Giovanni Tonietti. This work was supported by the PHRIENDS Specific Targeted Research Project, funded under the 6th Framework Programme of the European Community under Contract IST-045359. The authors are solely responsible for its content.

## REFERENCES

- [1] R. Filippini, S. Sen, G. Tonietti and A. Bicchi, "A Comparative Dependability Analysis of Antagonistic Actuation Arrangements for Enhanced Robotic Safety", *IEEE International Conference on Robotics and Automation*, ICRA, Rome, 2007.
- [2] R. Filippini, S. Sen and A. Bicchi, "Variable Impedance Actuation for Physical Human Cooperating Robots: a Comparative Analysis of Safety, Performance and Dependability", *IARP-IEEE/RAS-EURON Joint Workshop on Technical Challenges for Dependable Robots in Human Environments*, Rome, April 2007.
- [3] "International Standard Organization, Manipulating Industrial Robots - Performance Criteria and Related Test Methods", *ISO 9283*, 1998, Geneva.
- [4] J. Versace, "A Review of the Severity Index", *Proc. of the Fifteenth Stapp Car Crash Conference*, SAE Paper No. 710881, Society of Automotive Engineers, 1971, pp.771-796.
- [5] A. Bicchi and S. Lodi Rizzini and G. Tonietti, "Compliant Design for Intrinsic Safety: General Issues and Preliminary Design", *IROS*, 2001, Maui Hawaii.
- [6] A. Bicchi and G. Tonietti, "Design, Realization and Control of a Passively Compliant Robot for Intrinsic Safety", *Proc. Second IARP/IEEE-RAS Joint Workshop on Technical Challenge for Dependable Robots in Human Environments*, 2002.
- [7] A. Bicchi and G. Tonietti, "Fast and Soft Arm Tactics: Dealing with the Safety-Performance Tradeoff in Robot Arms Design and Control", *IEEE Robotics and Automation Magazine*, Vol. 11, No. 2, June, 2004.
- [8] M. Zinn and O. Khatib and B. Roth and J.K. Salisbury, "A New Actuation Approach for Human Friendly Robot Design", *Proc. of Int. Symp. on Experimental Robotics*, ISER, 2002.
- [9] G. Tonietti and R. Schiavi and A. Bicchi, "Design and Control of a Variable Stiffness Actuator for Safe and Fast Physical Human/Robot Interaction", *In Proc. IEEE Int. Conf. on Rob. & Aut.*, ICRA, 2005, pp.528-533.
- [10] G. Tonietti and R. Schiavi and A. Bicchi, "Optimal Mechanical/Control Design for Safe and Fast Robotics", *Proceedings of the 9th International Symposium on Experimental Robotics*, 18-21 June, Singapore, 2004.
- [11] G. Boccadamo, R. Schiavi, S. Sen, G. Tonietti, and A. Bicchi. "Optimization and Fail-Safety Analysis of Antagonistic Actuation for pHRI", *In European Robotics Symposium 2006, volume 22 of Springer Tracts in Advanced Robotics*, Henrik I. Christensen, editor, pages 109 - 118. Springer Berlin / Heidelberg, 2006.
- [12] F. Grashof, "Theoretische Maschinenlehre", *Leipzig*, 1883, pp.113-118.
- [13] W-T. Chang, C-C. Lin, and L-L. Wu, "A note on Grashof's Theorem", *J. of Marine Science and Tech.*, vol.13, no.4, 2005 pp.239-248.
- [14] J.W. Hurst, J.E Chestnutt, and A.A Rizzi, "An actuator with physically variable stiffness for highly dynamic legged locomotion", *Proc. IEEE International Conference on Rob & Aut.*, ICRA, 2004, April.
- [15] G.A. Pratt and M. Williamson, "Series elastics actuators", *IROS* 1995, pp.399-406.
- [16] S. Haddadin, A. Albu-Schffer, G. Hirzinger, "Dummy Crashtests for Evaluation of Rigid Human-Robot Impacts", *International Workshop on Technical Challenges for dependable robots in Human Environments*, 2007.